

Structure of 4-fluorophenol and barrier to internal –OH rotation in the S₁-state

Christian Ratzer, Michael Nispel and Michael Schmitt*

Institut für Physikalische Chemie, Universitätsstraße 26.43.02, D-40225 Düsseldorf, Germany

Received 16th October 2002, Accepted 15th January 2003

First published as an Advance Article on the web 29th January 2003

The structure and barrier to internal rotation of 4-fluorophenol in the ground state and the electronically excited S₁-state has been examined by resonantly enhanced two photon ionization spectroscopy and by rotationally resolved laser induced fluorescence spectroscopy of 4-fluorophenol and 4-fluorophenol-d₁. The rotationally resolved spectrum of the electronic origin of 4-fluorophenol is comprised of two subbands, which are split by 174.1 ± 0.5 MHz. From the splitting, determined from the HRLIF and several torsional bands observed in the R2PI spectrum an excited state barrier for the internal rotation of the hydroxy group of 1819.0 ± 5 cm⁻¹ was calculated. The subtorsional splitting of 4-fluorophenol-d₁ could not be resolved. The experimentally determined structural parameters from a fit to the rotational constants and the barrier to internal rotation in both electronic states are compared to the results of *ab initio* calculations. The molecule shows quinoidal distortion upon electronic excitation, with a shortening of both the C–O and the C–F bonds.

1 Introduction

The determination of the structure of aromatic molecules in electronically excited states allows insight into electronic effects upon electronic excitation. These electronic effects show up in molecular properties like excited state lifetimes, barriers to internal motions, and geometry changes in the molecule. Comparison of microscopic data like the barriers to internal rotation to macroscopic molecular properties like pK_a-values of substituted aromatics might provide relations for the straightforward determination of pK_a-values in different electronic states. In a recent study we examined the structure and the barrier to internal rotation of the hydroxy group of phenol in the first excited S₁-state. In order to study the electronic nature of the barrier to internal rotation we introduced substituents in the aromatic ring with various electronic influences. The first of these substances which we investigated using rotationally resolved LIF spectroscopy was 4-cyanophenol.¹ If we divide the substituents into groups as known from the theory of electrophilic aromatic substitution, the cyanogroup is representative for substituents with an electron withdrawing inductive (–I) and mesomeric effect (–M).

The present study is concerned with 4-fluorophenol, in which the fluorine atom exerts an electron withdrawing –I-effect too, but in contrast to 4-cyanophenol a +M-effect. The aim of this study is to investigate the influence of these electronic effects on the spectrum and especially on the torsional barrier in both electronic states. The torsional barrier of 4-fluorophenol in the electronic ground state has been determined by Larsen to be 1006 cm⁻¹ using microwave² and far-infrared spectroscopy.³ Up to now no experimental value for the S₁ barrier has been reported to our knowledge.

Cvitaš *et al.* examined structural changes of several mono- and disubstituted benzenes upon electronic excitation from their rotational band contours in the electronic spectra.^{4–7} Christoffersen *et al.*⁸ fitted the rotational constants of 4-fluoroaniline and 4-fluorophenol to the band contour in the electronic spectrum and reported the rotational constants of ground and excited electronic states.

2 Experimental setup

The experimental setup for the rotationally resolved LIF is described elsewhere.⁹ Briefly, it consists of a ring dye laser (Coherent 899-21) operated with Rhodamine 110, pumped with 6 W of the 514 nm line of an Ar⁺-ion laser (Coherent Innova 100). The light is coupled into an external folded ring cavity (LAS WaveTrain)¹⁰ for second harmonic generation (SHG). The molecular beam machine consists of three differentially pumped vacuum chambers that are linearly connected by skimmers. The expansion chamber is evacuated by a 8000 l s⁻¹ oil diffusion pump (Leybold DI 8000), which is backed by a 250 m³ h⁻¹ roots blower pump (Saskia RPS 250) and a 65 m³ h⁻¹ rotary pump (Leybold D65B). The second chamber serves as a buffer chamber and is pumped by a 400 l s⁻¹ turbo-molecular pump (Leybold Turbovac 361), backed by a 40 m³ h⁻¹ rotary pump (Leybold D40B), maintaining a chamber pressure below 1×10^{-5} mbar. The third chamber is pumped by a 145 l s⁻¹ turbo-molecular pump (Leybold Turbovac 151) through a liquid nitrogen trap and backed by a 16 m³ h⁻¹ rotary pump (Leybold D16B) resulting in a vacuum better than 1×10^{-6} mbar. The molecular beam is crossed at right angles with the laser beam 360 mm downstream of the nozzle. The resulting fluorescence is collected perpendicular to the plane defined by the laser and molecular beam by an imaging optics setup consisting of a concave mirror and two plano-convex lenses. The integrated molecular fluorescence is detected by a photo-multiplier tube (Thorn EMI 9863QB) whose output is discriminated and digitized by a photon counter (Stanford Research Systems SR400) and transmitted to a PC (Pentium II/233). Also the UV laser power, the iodine absorption spectrum and the interferometer transmission signal are detected by photo diodes and stored with the spectrum.

The experimental setup for the resonance enhanced two-photon ionization (R2PI) is explained in detail elsewhere.^{11,12} Briefly, the apparatus consists of a source chamber pumped with a 1000 l s⁻¹ oil diffusion pump (Alcatel) in which the molecular beam is formed by expanding a mixture of helium and 4-fluorophenol through the 500 μm orifice of a pulsed nozzle (General Valve, Iota One). The skimmed molecular beam

(Beam Dynamics Skimmer, 3 mm orifice) crosses the laser beams at right angles in the ionization chamber. The ions are extracted in a gridless Wiley–McLaren type time-of-flight (TOF) spectrometer (Bergmann Meßgeräte Entwicklung) perpendicular to the molecular beam and laser direction and enter the third (drift) chamber where they are detected using multi channel plates (Galileo). Ionization and drift chamber are both pumped with a 150 l s^{-1} rotatory pump (Leybold). The vacuum in the three chambers with the molecular beam on was 1×10^{-3} mbar (source), 5×10^{-5} mbar (ionization) and 1×10^{-7} mbar (drift), respectively. The resulting TOF signal was digitized by a 500 MHz oscilloscope (TDS 520A, Tektronix) and transferred to a personal computer, where the TOF spectrum was recorded and stored. The R2PI measurements were carried out using the frequency doubled output of a Nd:YAG (Spectra Physics, GCR170) pumped dye laser (LAS, LDL205) operated with Fluorescein 27.

4-Fluorophenol was purchased from Fluka and was used without further purification. 4-Fluorophenol- d_1 was prepared from 4-fluorophenol by refluxing with an excess of D_2O three times with subsequent removal of the solvent. This procedure resulted in an isotopic purity of $>95\%$.

3 Results and discussion

Fig. 1 shows part of the rotationally resolved LIF spectrum of the electronic origin $\tilde{\text{A}} \ ^1\text{B}_2 \leftarrow \tilde{\text{X}} \ ^1\text{A}_1$ of 4-fluorophenol at $35\,116.30 \text{ cm}^{-1}$. The spectrum is comprised of two subbands, which are of pure b -type and are separated by approximately 170 MHz. This splitting can be traced back to the hindered internal motion of the hydroxy group and will be discussed in detail in section 3.2. 4-Fluorophenol is a near prolate

asymmetric rotor in both electronic states as can be seen from its κ -value of -0.844 in the S_0 -state and -0.85 S_1 -state, *cf.* Table 1. The rotational temperature determined, taking nuclear spin statistics into account (*cf.* section 3.2) is 1.3 K. The S_1 state lifetime of 4-fluorophenol was determined from the Lorentzian contribution to the Voigt line shape to be $1.8 \pm 0.1 \text{ ns}$. This is close to the lifetime determined for phenol.

Fig. 2 shows the rotationally resolved LIF spectrum of the electronic origin of 4-fluorophenol- d_1 at $35\,108.87 \text{ cm}^{-1}$. The origin band of the deuterated isotopomer is red-shifted by 7.4 cm^{-1} , a value considerably larger than in phenol (1.8 cm^{-1}). The lifetime determined from the Lorentzian width of 49.7 MHz amounts to $3.2 \pm 0.1 \text{ ns}$, which is considerably shorter than the lifetimes obtained for all OD-isotopomers of phenol. The torsional subbands could not be resolved for the deuterated isotopomer. Because the torsional splitting in the electronic ground state, determined by microwave spectroscopy amounts only to 1.16 MHz,² we were not able to resolve the splitting, with a Gaussian contribution to the line width of 20 MHz and a Lorentzian width of 50 MHz.

3.1 Rotational constants

The inertial parameters of 4-fluorophenol and 4-fluorophenol- d_1 have been determined by a fit of the rovibronic transitions to a rigid rotor Hamiltonian. The maximum J -value, which could be detected in our jet-cooled spectrum is $J = 10$. Therefore inclusion of centrifugal distortion constants do not improve the fit of the inertial parameters to our rovibronic transitions. The ground state rotational constants have been

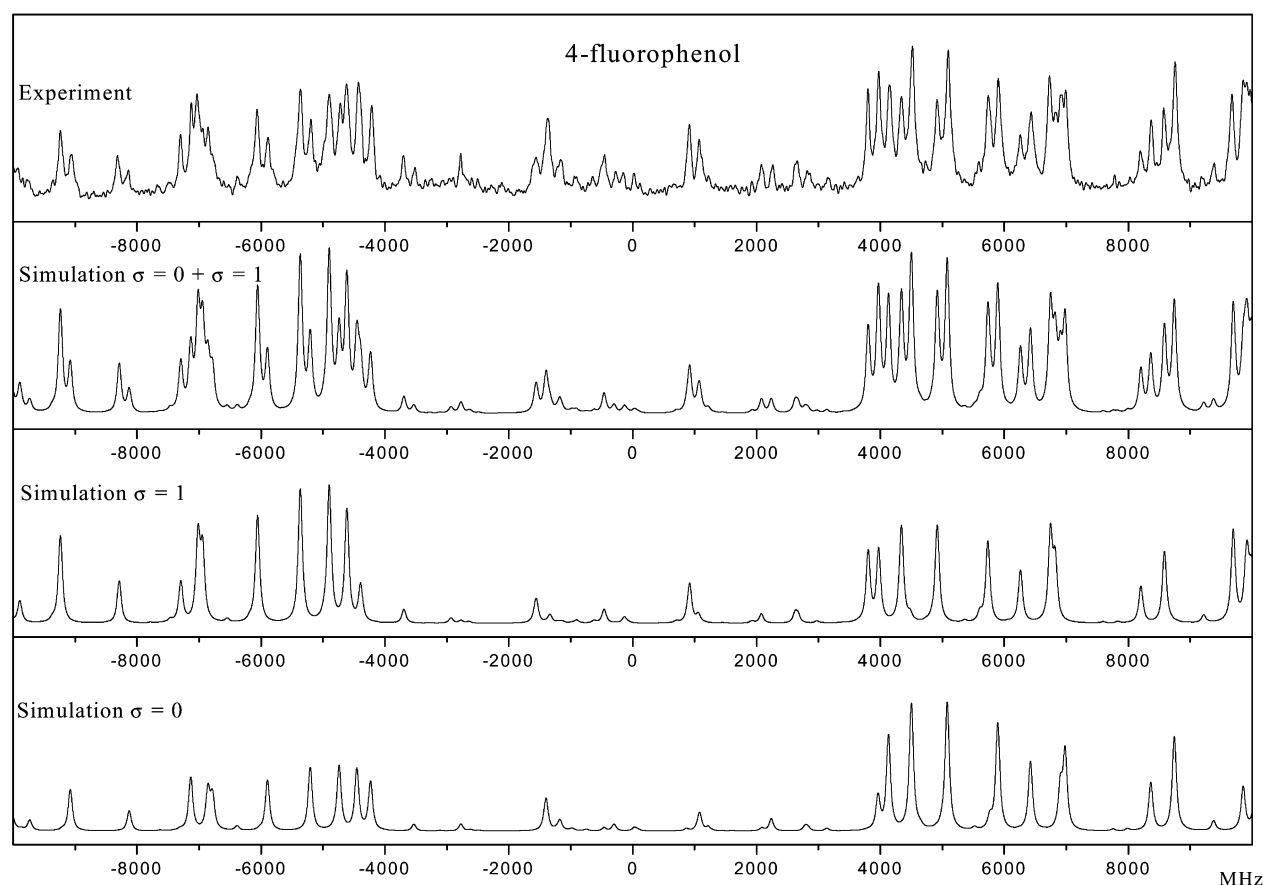


Fig. 1 Part of the rotationally resolved spectra of the electronic origin of 4-fluorophenol together with the simulation of the two torsional subbands. The subbands are labeled with 0^+ for the $\sigma = 0$ component of the vibronic ground state and with 0^- for the $\sigma = 1$ component.

Table 1 Molecular constants of 4-fluorophenol and 4-fluorophenol- d_1 obtained from the fit to the experimental spectra. The number of digits retained for each parameter were calculated according to the scheme of Watson,²⁴ so that the calculated line frequencies can be reproduced within 10% of their standard deviation; the ground state rotational constants have been obtained from a fit of the microwave transitions from ref. 2 to a rigid rotor Hamiltonian

	4-Fluorophenol	4-Fluorophenol- d_1
A'' /MHz	5625.594(8)	5584.315(7)
B'' /MHz	1454.6877(45)	1414.340(3)
C'' /MHz	1156.0073(39)	1128.758(3)
$\Delta I/u \text{ \AA}^2$	-0.0734(22)	-0.0947
κ	-0.86634(3)	-0.87181
A' /MHz	5268.0(1)	5231.546(42)
B' /MHz	1473.65(8)	1433.3650(74)
C' /MHz	1152.54(4)	1125.7998(47)
$\Delta I/u \text{ \AA}^2$	-0.528(22)	-0.277(2)
κ	-0.844	-0.85
$\tilde{\nu}/\text{cm}^{-1}$	35 116.30(1)	35 108.87(1)
$t_{1/2}/\text{ns}$	1.8(1)	3.2(1)
$\Delta\nu_{\text{sub}}/\text{MHz}$	174.1(5)	-
Lines	44	101
$S(y)/\text{MHz}$	4.0	2.5

fit to experimental microwave transitions[†] using the same rigid rotor Hamiltonian and have subsequently been kept fixed in our fit of the rovibronic transitions. Because we want to elucidate geometry changes upon electronic excitation the use of the same Hamiltonian for both electronic states is crucial. The range of microwave transitions used in the fit of the ground state rotational constants has been selected to match the range observed in the jet-cooled LIF-spectrum ($J_{\text{max}} \leq 10$). The deviations of the fit from a rigid rotor Hamiltonian compared to the fit given by Larsen,² which includes four centrifugal distortion constants, is smaller than 0.02 MHz. This value is considerably smaller than the uncertainties of our excited state rotational constants. The A rotational constant of 4-fluorophenol decreases by 357.6 MHz upon electronic excitation, B increases by 18.9 MHz and C decreases by 3.5 MHz close to the values determined by Christoffersen *et al.*⁸ from a rotational band contour analysis (-374.7 MHz, +21.9 MHz, -3.3 MHz). The changes of the rotational constants of 4-fluorophenol- d_1 are -352.8, +19.0, and -3.0 MHz, respectively. These constants will be used in section 3.3 to derive the structural changes upon electronic excitation.

3.2 The vibronic spectrum

The torsional splitting ($0^+/0^-$) of 4-fluorophenol in the electronic ground state has been determined by microwave spectroscopy to be 177.121 MHz.² Larsen and Nicolaisen³ determined the torsional transitions $1^\pm \leftarrow 0^\pm$, $2^+ \leftarrow 1^+$, $2^- \leftarrow 1^-$, $3^+ \leftarrow 2^+$, and $3^- \leftarrow 2^-$ to be 279.1, 243.3, 247.1, 187.9, and 219.6 cm^{-1} respectively. From these transitions and the $0^+/0^-$ splitting a barrier to internal rotation in the electronic ground state of 1006 cm^{-1} was calculated. This is considerably lower than the ground state barrier in phenol (1215 cm^{-1})¹³ and 4-cyanophenol (1420 cm^{-1}).¹

The line splitting observed in the LIF spectrum amounts to 174.1 ± 0.5 MHz, *cf.* Table 1. Together with the selection rule $\Delta\sigma = \pm 1$, the torsional level splitting in the electronically excited state can be determined to be 3.0 ± 0.5 MHz. Using this value and a torsional constant F of 690 GHz (as in the electronic ground state), the torsional S_1 -barrier is calculated to be 1816 ± 40 cm^{-1} . If we compare this value to the S_1 -barrier of

phenol (4710 ± 30 cm^{-1}), we find a substantial reduction by a factor of 2.6, while the S_0 -barrier drops only by a factor of 1.2.

Using this barrier one can predict higher torsional transitions and by a comparison to the vibronic spectrum further refine the value for the barrier and include the torsional constant in the fit. Fig. 3 shows the R2PI spectrum of 4-fluorophenol in the range of 0–1500 cm^{-1} , relative to the electronic origin at 35 116.3 cm^{-1} . The spectrum is similar to that already published by Tembreull *et al.*¹⁴ and Fujimaka *et al.*¹⁵ but we had to remeasure it in order to get the exact frequencies of all rovibronic bands, not quoted in the cited literature.

The allowed $2^\pm \leftarrow 0^\pm$ transition is calculated between 730 and 750 cm^{-1} using the uncertainty of the torsional barrier obtained from the high resolution experiment. In the vibronic spectrum the only transition in this range is found at 736.6 cm^{-1} which therefore can tentatively be assigned to this torsional transition. Using the $0^+/0^-$ splitting together with the frequency of the $2^\pm \leftarrow 0^\pm$ transition, we predict the frequency of $4^+ \leftarrow 0^+$ to be 1341 cm^{-1} and of $4^- \leftarrow 0^-$ to be 1354 cm^{-1} , in close agreement with experimental transitions at 1342.6 and 1361.4 cm^{-1} . Inclusion of the torsional constant F into the fit resulted in the torsional transition frequencies given in Table 2. The value of the barrier height from this fit is 1819.0 ± 5 cm^{-1} , for the torsional constant F a value of 683 ± 1 GHz is found, slightly smaller than in the electronic ground state.

The G_4 -symmetric 4-fluorophenol exhibits a 10:6 spin statistic for $K_a(\text{even}):K_a(\text{odd})$ for transitions of the torsional ground state $\sigma = 0$, and 6:10 for the torsionally excited state. In the fit of the torsional bands shown in Fig. 1 these spin statistics have been considered and reproduce the observed intensities at the rotational temperature of 1.3 K well.

The complete list of observed frequencies and relative intensities in the vibronic spectrum of 4-fluorophenol is given in Table 3. The transitions were assigned tentatively on the basis of *ab initio* calculations described in section 3.4.3.

3.3 Determination of the structure

The structure of 4-fluorophenol in the S_0 - and S_1 -state has been obtained from the fit of a model geometry to the rotational constants of 4-fluorophenol and 4-fluorophenol- d_1 , using the program pKRFit.¹⁶ Fig. 4 shows the model used for the fit and the atomic numbering. The molecule is supposed to be planar in both electronic states. Because *para*-disubstituted aromatics show a quinoidal distortion upon electronic excitation,⁷ we applied a model in which the C_1C_2 bond length is allowed to differ from C_2C_3 . In addition the C_4F distance has been fit.

The CCC and CCH angles in the aromatic have been set to 120° , the CH bond lengths to the benzene values and the CO and OH bond lengths to the values of phenol. The result of the fit of the r_0 -structure to the rotational constants of both isotopomers in the S_0 - and S_1 -state is shown in Table 4. In the S_0 -state the geometry of the aromatic is benzenoid, with equal bond lengths between C_1C_2 and C_2C_3 although they were not constrained equal in the fit. The C_4F bond length was determined to be 133.5 pm. In the S_1 -state the C_1C_2 and C_2C_3 bond lengths are determined to be different, with a marked quinoidal structure. The C_4F bond length decreases by 6 pm upon electronic excitation. Both effects are reproduced by the *ab initio* calculations, given for comparison in Table 4, although less pronounced. Certainly the restriction of CO and OH bond length to the values determined in phenol imposes a model error on the structural determination, which exceeds the propagated uncertainties of the rotational constants, given as uncertainties in Table 4.

In addition, we determined the position of the hydroxylic H-atom *via* a Kraitchman analysis. The moments of inertia which

[†] The experimental frequencies of the microwave transitions from ref. 2 have been made available to us by Prof. Larsen.

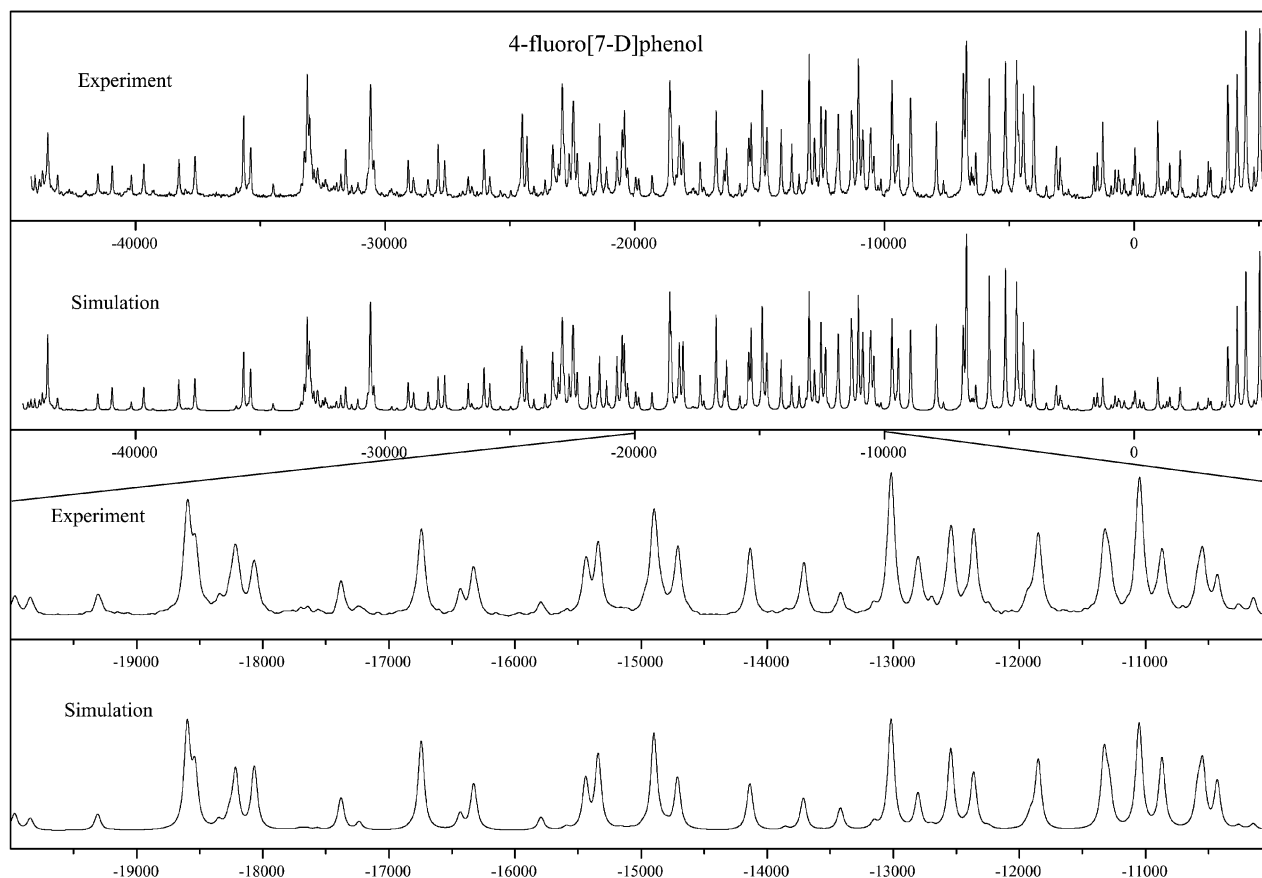


Fig. 2 Rotationally resolved spectra of the electronic origin of 4-fluorophenol-d₁, together with a simulation.

are used in the Kraitchman equations of the planar 4-fluorophenol are calculated from the A and B rotational constants.

Inspection of Table 5 shows, that the value of the a -coordinate of the hydroxylic H-atom of 4-fluorophenol decreases by

4.3 pm, and the b -coordinate slightly increases by 0.2 pm upon electronic excitation, while for phenol a and b increase by 0.5 and 1.1 pm, respectively. Because the heavy fluorine atom is located nearly at the a -axis, the very similar b -coordinate observed is as expected.

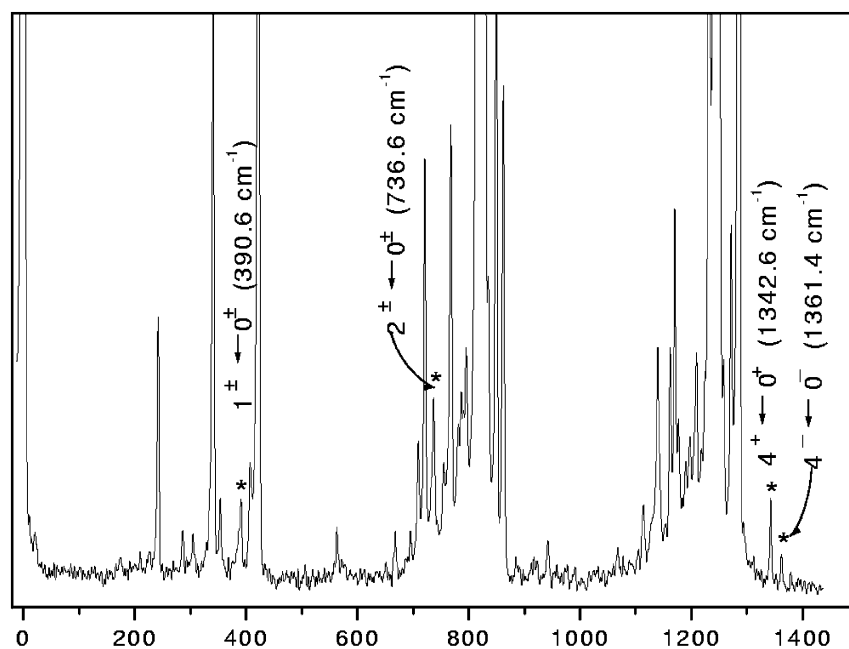


Fig. 3 R2PI spectrum 4-fluorophenol in the range of 0–1500 cm^{-1} , relative to the electronic origin at 35 116.3 cm^{-1} . The bands marked with an asterisk are the torsional bands, which have been used in the fit of the barrier (*cf.* text).

Table 2 Experimental and calculated torsional transitions (in cm^{-1}) of 4-fluorophenol using a V_2 barrier of 1819.0 cm^{-1} and a torsional constant of 22.81 cm^{-1} (683 GHz)

	Observed/ cm^{-1}	Calculated/ cm^{-1}
$0^+ \leftarrow 0^+$	0	0
$0^- \leftarrow 0^-$	1.001×10^{-4}	1.001×10^{-4}
$1^\pm \leftarrow 0^\pm$	390.6	383.1
$2^\pm \leftarrow 0^\pm$	736.6	739.2
$3^\pm \leftarrow 1^\pm$	786.0	785.4
$3^\pm \leftarrow 0^\pm$	1066.0	1064.0
$4^+ \leftarrow 0^+$	1342.6	1341.6
$4^- \leftarrow 0^-$	1361.4	1360.9

3.4 Comparison to the results of *ab initio* calculations

3.4.1 Structure. The structure of 4-fluorophenol in the electronic ground state has been calculated at the HF/6-311++G(d,p), B3LYP/6-311++G(d,p), and MP2/6-311++G(d,p) level and at the CIS/6-311++G(d,p) level for the electronically excited S_1 -state with the Gaussian 98 program package.¹⁷ The SCF convergence criterion used for our calculations was an energy change below $10^{-8} E_h$, while the convergence criterion for the gradient optimization of the molecular geometry was $\partial E/\partial r > 1.5 \times 10^{-5} E_h a_0$ and $\partial E/\partial \varphi > 1.5 \times 10^{-5} E_h \text{ degree}^{-1}$, respectively.

Table 6 gives the geometry parameters, obtained at various levels of theory. All structures have been proven to be minima *via* a normal mode analysis based on the analytical gradients. Table 7 compares the experimental rotational constants with the results of the *ab initio* calculations. The agreement of the experimental ground state constants with the results of the MP2 and B3LYP calculations is very good, while HF fails to describe the geometry correctly. The excited state rotational constants are reproduced poorly at the CIS level, as could be expected, regarding the deviations of the HF calculations for the ground state. Nevertheless, the change of the rotational constants upon electronic excitation is reproduced very well

Table 3 Experimental vibronic frequencies and relative intensities of 4-fluorophenol relative to the electronic origin at $35\,116.3 \text{ cm}^{-1}$; for the description of the modes see section 3.4.3

Transition	Frequency/ cm^{-1}	Relative intensity
Origin	0	100
$16a_0^2$	242.2	11
$\delta(\text{C-F})$	340.4	25
$6a_0^1$	422.2	47
	708.8	6
	720.8	20
$2^\pm \leftarrow 0^\pm$	736.6	7
$18a_0^1$	768.2	20
1_0^1	818.6	93
12_0^1	827.6	89
$6a_0^2$	834.8	12
	849.8	31
	862.0	21
	1140.0	10
	1162.0	10
$9a_0^1$	1170.4	16
	1209.2	8
$6a_0^3$	1231.6	37
$19a_0^1$	1240.6	79
$\delta(\text{CO-H})$	1249.0	87
	1271.4	14
$\nu(\text{C-O})$	1285.4	66
$4^- \leftarrow 0^-$	1342.6	4
$4^+ \leftarrow 0^+$	1361.4	4

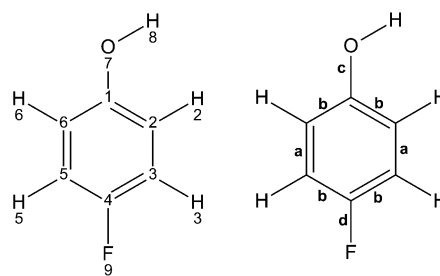


Fig. 4 Atomic numbering of 4-fluorophenol and model used for the fit of the geometry.

as the difference of CIS and HF calculations due to a favorable compensation of errors.

The position of the hydroxylic H-atom in the inertial system, obtained from the MP2/6-311++G(d,p) calculation is $a = 315.7 \text{ pm}$ and $b = 83.6 \text{ pm}$, close to the values determined from the Kraitchman analysis (312.8 and 79.38 pm). The position in the S_1 state calculated at the CIS/6-311++G(d,p) level is $a = 312.1 \text{ pm}$ and $b = 81.9 \text{ pm}$, reflecting the decrease of the a -coordinate found in the experiment.

3.4.2 Barrier to internal rotation. The transition state for the internal rotation, in which the OH-group is perpendicular relative to the aromatic ring, was optimized by the synchronous transit-guided quasi-Newton method (STQN),^{18,19} implemented in the Gaussian 98 program package.¹⁷ A normal mode analysis has been performed utilizing the analytical second derivatives of the potential energy surface both at the ground state and at the transition state. Table 8 gives the calculated barrier to internal rotation as the difference of the fully optimized equilibrium and transition state energies for the S_0

Table 4 Experimental r_0 -geometry parameters (distances in pm and angles in degrees) of 4-fluorophenol, obtained from a fit of the geometry to the experimental inertial parameters. Only the parameters with an asterisk have been optimized in the fit procedure; the *ab initio* geometry parameters, obtained with the 6-311G++(d,p) basis are given for comparison

	pKrFit S_0	MP2	pKrFit S_1	CIS
$C_1C_2^*$	139.89(9)	139.74	145.18(3)	142.54
$C_2C_3^*$	139.89(7)	139.83	139.5(50)	141.55
C_4F^*	133.56(13)	135.88	127.6(90)	131.47
C_1O	133.15	137.38	128.15	131.74
OH	96.6	96.52	96.6	94.7
$C_{ar}H$	108.1	108.1	107.1	107.1
$C_{ar}C_{ar}C_{ar}$	120	120	120	120
$C_{ar}C_{ar}H$	120	120	120	120
C_3C_4F	120	120	120	120
C_2C_1O	120	120	120	120
C_1OH	110	110	110	111
(obs – calc)/MHz	0.26	–	0.47	–

Table 5 Substitution coordinates (in pm) of the H-atom in 4-fluorophenol and phenol for both electronic states

	S_0		S_1	
	a	b	a	b
4-Fluorophenol	312.84(9)	79.38(12)	308.51(10)	79.60(12)
Phenol	258.6(1)	85.3(2)	259.1(2)	86.4(3)

Table 6 *Ab initio* structural parameters of 4-fluorophenol; rotational constants are given in MHz, distances in pm, angles and dihedral angles in degrees

	6-31G(d,p)				6-311++G(d,p)			
	HF	B3LYP	MP2	CIS	HF	B3LYP	MP2	CIS
<i>A</i> /MHz	5736	5627	5623	5396	5745	5646	5607	5397
<i>B</i> /MHz	1475	1447	1447	1499	1477	1449	1446	1505
<i>C</i> /MHz	1173	1151	1151	1173	1175	1153	1149	1177
<i>C</i> ₁ <i>C</i> ₂	138.43	139.86	139.74	141.85	138.32	139.54	139.99	142.23
<i>C</i> ₂ <i>C</i> ₃	138.78	139.60	139.64	140.77	138.81	139.48	140.04	140.37
<i>C</i> ₃ <i>C</i> ₄	137.35	138.80	138.78	140.47	137.20	138.38	138.98	140.43
<i>C</i> ₄ <i>C</i> ₅	138.00	139.11	139.07	140.12	137.86	138.70	139.24	140.22
<i>C</i> ₅ <i>C</i> ₆	138.10	139.23	139.26	140.92	138.13	139.10	139.69	140.50
<i>C</i> ₂ <i>H</i> ₂	107.69	108.76	108.41	107.42	107.67	108.56	108.80	107.40
<i>C</i> ₃ <i>H</i> ₃	107.41	108.44	108.10	107.15	107.41	108.27	108.51	107.17
<i>C</i> ₃ <i>H</i> ₅	107.42	108.45	108.10	107.12	107.42	108.28	108.52	107.14
<i>C</i> ₆ <i>H</i> ₆	107.41	108.45	108.14	107.16	107.40	108.29	108.55	107.18
<i>C</i> ₁ <i>O</i>	135.32	136.88	137.38	132.62	133.12	137.07	137.14	131.98
<i>C</i> ₄ <i>F</i>	133.40	135.30	135.88	131.81	135.29	135.91	135.29	131.05
<i>OH</i>	94.25	96.59	96.52	94.45	94.04	96.26	96.24	94.30
<i>C</i> ₁ <i>C</i> ₂ <i>C</i> ₃	120.1896	120.1994	120.0631	118.2500	120.1936	120.1558	120.1893	118.205
<i>C</i> ₂ <i>C</i> ₃ <i>C</i> ₄	119.0720	119.0209	118.8672	117.7106	119.0556	118.8458	118.7677	117.8879
<i>C</i> ₃ <i>C</i> ₄ <i>C</i> ₅	121.5544	121.5997	121.8908	124.8907	121.5687	121.9024	121.9114	124.7542
<i>C</i> ₄ <i>C</i> ₅ <i>C</i> ₆	119.2368	119.2213	119.0029	117.4762	119.2413	119.0585	118.9800	117.5073
<i>C</i> ₁ <i>C</i> ₂ <i>H</i> ₂	120.2133	120.0986	120.1923	120.2286	120.2685	119.6325	120.1512	120.1345
<i>C</i> ₂ <i>C</i> ₃ <i>H</i> ₃	121.1419	121.2501	121.4084	122.7545	121.0189	121.2039	121.3014	122.6564
<i>C</i> ₃ <i>C</i> ₄ <i>F</i>	119.3262	119.2218	119.0667	117.3608	119.3197	119.0646	119.0487	117.4726
<i>C</i> ₄ <i>C</i> ₅ <i>H</i> ₅	119.5786	119.5463	119.5963	119.7497	119.6962	119.7684	119.7334	119.7471
<i>C</i> ₅ <i>C</i> ₆ <i>H</i> ₆	120.9520	121.0110	121.1353	122.5505	120.7987	120.8678	120.8518	122.4492

(HF, B3LYP, MP2). Barriers for phenol and 4-cyanophenol are given for comparison. The value of the torsional barrier depends critically on the truncation of the basis set and the order of the perturbation correction to the SCF energy as has been shown by Kim and Jordan²⁰ for phenol. As one can see from Table 8, the more flexible the basis, the lower is the barrier given one method. Therefore we also employed a complete basis set method (CBS)²¹ combined with higher order corrections for the perturbation series, as described by Ochterski *et al.*²² (CBS-Q) to calculate the ground state barrier of 4-fluorophenol. The best agreement between experiment and theory can be found for B3LYP/6-311++G(d,p) and the CBS-Q model chemistry. Interestingly, the theoretical value is larger than the calculated barrier using CBS-Q. In the case of phenol Kim and Jordan²⁰ found a theoretical barrier at the QCISD(T)/6-31++G(2df,p) level of theory which is 131 cm⁻¹ smaller than the experimental value. They attributed this difference mainly to different definitions of the barrier. While the experimental barrier is determined assuming a rigid frame and rotor model, both geometries are allowed to relax in the determination of the theoretical barrier. This should lower the calculated barrier relative to the experimental value. Kim and Jordan²⁰ estimated this difference to be about 70 cm⁻¹. Another difference is the inclusion of zero-point vibrational effects from coordinates other than the torsion in the experimentally determined value. We performed a normal mode analysis for each level of theory given in Table 8. Independent of method and basis set applied, the difference in zero-point

Table 7 Comparison of *ab initio* rotational constants of 4-fluorophenol, obtained with the 6-311++G(d,p) basis set with the experiment

	Exp.			Exp.			CIS – HF
	(<i>S</i> ₀)	HF	B3LYP	(<i>S</i> ₁)	CIS	(<i>S</i> ₁ – <i>S</i> ₀)	
<i>A</i>	5625.5	5745	5646	5623	5268.0	5397	–357.6
<i>B</i>	1454.7	1477	1449	1447	1473.6	1505	+18.9
<i>C</i>	1156.0	1175	1153	1151	1152.5	1177	–3.5

energy between equilibrium geometry and transition state amounts to 15–20 cm⁻¹ the zero-point energy of the transition state being smaller than of the equilibrium structure. Therefore this effect tends to raise the calculated barrier relative to the experimental one. A third effect on the value of the barrier, which was considered by Kim and Jordan²⁰ is the neglect of higher terms in the Fourier expansion:

$$V(\phi) = \sum_{n=1}^{\infty} \frac{V_{2n}}{2} [1 - \cos(2n\phi)] \quad (1)$$

in the determination of the experimental barrier. If we introduce a *V*₄-term into the fit of the vibronic transitions, we obtain a *V*₂-barrier only 10 cm⁻¹ lower and a *V*₄-term of 26 cm⁻¹. Thus, assessing the deviations between the experimental and the theoretical barrier, by far the largest effect is the relaxation of all molecular coordinates other than the torsion in the course of the calculation. Zero-point effects, and the inclusion of higher terms in the Fourier expansion (1) lead to errors of about one order of magnitude less.

The electronically excited *S*₁ state has been calculated at the CIS and time dependent (TD) DFT level. The excited state barrier is determined from the results of the CIS and TD-DFT calculations *via*:

$$[E_{\text{equilibrium}}(\text{RHF}) + E_{\text{equilibrium}}(\text{excitation})] - [E_{\text{trans state}}(\text{RHF}) + E_{\text{trans state}}(\text{excitation})] \quad (2)$$

where *E*(excitation) is the excitation energy of the lowest excited singlet state for the equilibrium structure and the transition state, respectively and *E*(RHF) are the respective Hartree–Fock energies. Regarding the fact that HF reproduces the ground state barriers very poorly, it cannot be expected, that CIS gives much better values for the *S*₁ state. Nevertheless, an increase of the barrier height upon electronic excitation is found in the calculation, although the absolute value shows very large deviations. Also the barrier calculated at the time dependent DFT level shows unacceptable large deviation from the experiment.

Table 8 Experimental and calculated barriers to internal rotation of 4-fluorophenol, phenol, and 4-cyanophenol

State	Method	4-Fluorophenol		Phenol		4-Cyanophenol	
		$V_{2,e}$	$V_{2,0}$	$V_{2,e}$	$V_{2,0}$	$V_{2,e}$	$V_{2,0}$
S_0	Experiment	1006	–	1215	–	1420	–
	HF/6-31G(d,p)	652	486	905	716	1192	963
	HF/6-311++G(d,p)	596	463	846	691	1127	931
	B3LYP/6-31G(d,p)	1176	969	1387	1169	1682	1426
	B3LYP/6-311++G(d,p)	1030	870	1224	1054	1508	1297
	MP2/6-31G(d,p)	1036	869	1209	1028	1393	1187
	MP2/6-311++G(d,p)	843	443	1033	965	1205	1080
	CBS-Q	1054	881	–	–	–	–
S_1	Experiment	1820	–	4710	–	≥ 5000	–
	CIS/6-31G(d,p)	2337	2178	2061	1978	2133	2226
CIS/6-311++G(d,p)	2684	2180	2354	2248	2140	2248	–
	B3LYP-TD/6-311++G(d,p)	3490	–	3211	–	2714	–

3.4.3 Vibrations. Table 9 shows the harmonic frequencies, calculated at the CIS/6-311++G(d,p) level of theory. The designation of the modes follows the nomenclature of Varsanyi.²³ The torsional mode τ mixes strongly to several modes, in particular to the low frequency out of plane modes 16a, 16b, and 11. The Varsanyi modes 15 and 9b are indistinguishable due to the similar masses of the fluorine and the hydroxy substituent, one being the C–F bending mode, the other the C–O bending mode. Comparison of the calculated harmonic modes with the experimental frequencies leads to the assignment of the vibronic transitions given in Table 3. This very tentative assignment for the vibronic bands has to be checked against dispersed

fluorescence data, using the propensity rule, as an additional guidance in the assignment.

4 Conclusion

The change of the structure of 4-fluorophenol upon electronic excitation was investigated by high resolution LIF spectroscopy of two isotopomers of the compound. Both experiment and *ab initio* theory predict a benzenoid structure in the electronic ground state, but a quinoidal distortion along the long molecular axis in the S_1 state. The CF and CO bond lengths were both found to decrease upon electronic excitation. The change of the inertial parameters upon electronic excitation can be predicted with high accuracy from the difference of the CIS and the HF rotational constants. Although the close agreement between experiment and theory is mainly due to a cancelation of errors, it proves very helpful to get a first guess for the rotational constants in the S_1 state.

The barrier to internal rotation of the hydroxy group in 4-fluorophenol increases from 1006 cm^{-1} in the S_0 -state to 1819 cm^{-1} in the electronically excited S_1 -state, while the barriers in phenol increase from 1215 to 4710 and in 4-fluorophenol from 1420 to ≥ 5000 cm^{-1} . The increase in barrier height can be attributed to a transfer of electron density from the hydroxy group into the aromatic ring upon electronic excitation, which is reflected in the shorter bond length and the expansion of the aromatic ring in the S_1 state. A partially quinoidal structure is formed in the S_1 state with an increased bond order between the hydroxylic oxygen and the ring carbon atom. The same holds true for phenol and for 4-cyanophenol, but the resulting negative partial charge in 4-fluorophenol cannot be efficiently delocalized as in the case of 4-cyanophenol due to the +M effect of the fluorine substituent. Therefore the increase in barrier height upon electronic excitation in 4-fluorophenol is the smallest of the three phenols.

Acknowledgements

This work was made possible by the support of the Deutsche Forschungsgemeinschaft (SCHM 1043/9-2). We gratefully acknowledge the support of Prof. Dr. Karl Kleinermanns. We thank Prof. N. W. Larsen for placing the frequencies of the microwave transitions of 4-fluorophenol at our disposal. The help of Petra Imhof in recognizing the Varsanyi modes and of Isabel Hünig for experimental help with the R2PI spectrum are gratefully acknowledged.

Table 9 Calculated vibrational frequencies of 4-fluorophenol in the S_0 and the S_1 state

Number	Mode		CIS 6-311++G(d,p)
1	16a	o.o.p.	95
2	11	o.o.p.	143
3	16b [τ (OH)]	o.o.p.	299
4	τ (OH) [16b]	o.o.p.	315
5	δ (C–F) [15]	i.p.	387
6	δ (C–OH) [9b]	i.p.	449
7	6a	i.p.	466
8	17b	o.o.p.	545
9	10a	o.o.p.	563
10	17a	o.o.p.	613
11	6b	i.p.	621
12	4	o.o.p.	623
13	10b	o.o.p.	760
14	5	o.o.p.	768
15	18a	i.p.	802
16	1	i.p.	910
17	12	i.p.	1067
18	18b	i.p.	1137
19	δ (CO–H)	i.p.	1224
20	9a	i.p.	1239
21	ν (C–F)	i.p.	1379
22	19b	i.p.	1404
23	ν (C–O)	i.p.	1436
24	3	i.p.	1487
25	8b	i.p.	1551
26	19a	i.p.	1625
27	8a	i.p.	1769
28	14	i.p.	1831
29	ν (C–H)	i.p.	3365
30	ν (C–H)	i.p.	3400
31	ν (C–H)	i.p.	3409
32	ν (C–H)	i.p.	3417
33	ν (O–H)	i.p.	4172

References

- 1 J. Küpper, M. Schmitt and K. Kleinermanns, *Phys. Chem. Chem. Phys.*, 2002, **4**, 4634.
- 2 N. W. Larsen, *J. Mol. Struct.*, 1986, **144**, 83.
- 3 N. W. Larsen and F. M. Nicolaisen, *J. Mol. Struct.*, 1974, **22**, 29.
- 4 T. Cvitaš and J. Hollas, *Mol. Phys.*, 1970, **18**, 101.
- 5 T. Cvitaš and J. Hollas, *Mol. Phys.*, 1970, **18**, 793.
- 6 T. Cvitaš and J. Hollas, *Mol. Phys.*, 1970, **18**, 801.
- 7 T. Cvitaš, J. Hollas and G. Kirby, *Mol. Phys.*, 1970, **19**, 305.
- 8 J. Christoffersen, J. M. Hollas and G. H. Kirby, *Mol. Phys.*, 1970, **18**, 451.
- 9 M. Schmitt, J. Küpper, D. Spangenberg and A. Westphal, *Chem. Phys.*, 2000, **254**, 349.
- 10 M. Okruss, R. Müller and A. Hese, *J. Mol. Spectrosc.*, 1999, **193**, 293.
- 11 M. Schmitt, C. Jacoby and K. Kleinermanns, *J. Chem. Phys.*, 1998, **108**, 4486.
- 12 W. Roth, C. Jacoby, A. Westphal and M. Schmitt, *J. Phys. Chem. A*, 1998, **102**, 3048.
- 13 G. Berden, W. L. Meerts, M. Schmitt and K. Kleinermanns, *J. Chem. Phys.*, 1996, **104**, 972.
- 14 R. Tembreull, T. M. Dunn and D. M. Lubman, *Spectrochim. Acta A*, 1986, **42**, 899.
- 15 E. Fujimaki, A. Fujii, T. Ebata and N. Mikami, *J. Chem. Phys.*, 1999, **110**, 4238.
- 16 C. Ratzer, J. Küpper, D. Spangenberg and M. Schmitt, *Chem. Phys.*, 2002, **283**, 153.
- 17 M. J. Frisch, G. W. Trucks, H. B. Schlegel, G. E. Scuseria, M. A. Robb, J. R. Cheeseman, V. G. Zakrzewski, J. A. Montgomery Jr., R. E. Stratmann, J. C. Burant, S. Dapprich, J. M. Millam, A. D. Daniels, K. N. Kudin, M. C. Strain, O. Farkas, J. Tomasi, V. Barone, M. Cossi, R. Cammi, B. Mennucci, C. Pomelli, C. Adamo, S. Clifford, J. Ochterski, G. A. Petersson, P. Y. Ayala, Q. Cui, K. Morokuma, D. K. Malick, A. D. Rabuck, K. Raghavachari, J. B. Foresman, J. Cioslowski, J. V. Ortiz, A. G. Baboul, B. B. Stefanov, G. Liu, A. Liashenko, P. Piskorz, I. Komaromi, R. Gomperts, R. L. Martin, D. J. Fox, T. Keith, M. A. Al-Laham, C. Y. Peng, A. Nanayakkara, C. Gonzalez, M. Challacombe, P. M. W. Gill, B. Johnson, W. Chen, M. W. Wong, J. L. Andres, C. Gonzalez, M. Head-Gordon, E. S. Replogle and J. A. Pople, *Gaussian 98 Revision A.7*, Gaussian, Inc., Pittsburgh, PA, 1998.
- 18 C. Peng, P. Y. Ayala, H. B. Schlegel and M. J. Frisch, *J. Comput. Chem.*, 1996, **17**, 49.
- 19 C. Peng and H. B. Schlegel, *Isr. J. Chem.*, 1994, **33**, 449.
- 20 K. Kim and K. D. Jordan, *Chem. Phys. Lett.*, 1994, **218**, 261.
- 21 M. R. Nyden and G. A. Petersson, *J. Chem. Phys.*, 1981, **75**, 1843.
- 22 J. W. Ochterski, G. A. Petersson and J. A. Montgomery, *J. Chem. Phys.*, 1996, **104**, 2598.
- 23 G. Varsanyi, *Assignments for Vibrational Spectra of 700 Benzene Derivatives*, Wiley, New York, 1974.
- 24 J. K. G. Watson, *J. Mol. Spectrosc.*, 1977, **66**, 500.